Supporting Information

Lucas et al. 10.1073/pnas.1405391111

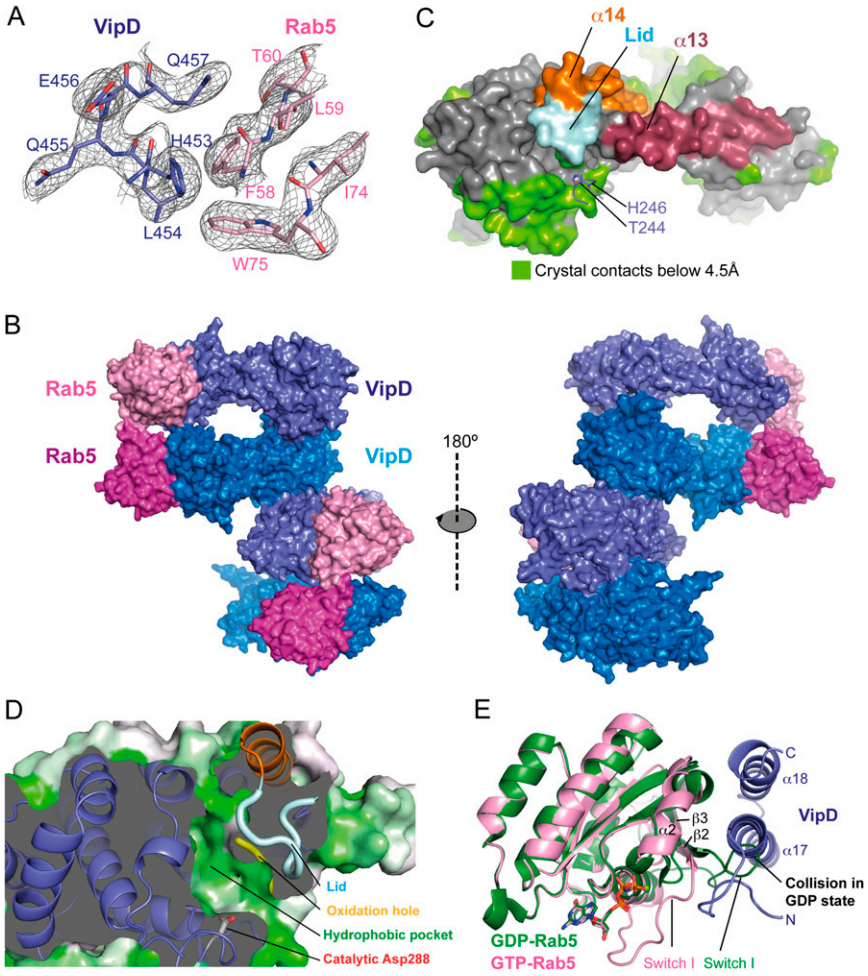

Fig. S1. (*A*) Electron density map (2Fo-Fc) calculated with phases derived from the final refined model and contoured at 1.5 sigma in the vicinity of the VipD-Rab5c interface. (*B*) Packing of four VipD–Rab5 complexes that form an asymmetric unit. VipD is colored in blue/slate; Rab5 is in light and dark pink. (*C*) Distribution of VipD surface areas with crystal lattice contacts below 4.5 Å (same orientation as in Fig. 2 *C*–*E*). Note that there are no mayor crystallographic contacts in areas corresponding to α13, α14, and the lid except for two residues (Thr244 and His246) from a symmetrically related VipD molecule that are partially inserted at the edge of the catalytic groove, most probably favored by the opening of the lid. The symmetrically related VipD molecule is omitted from the figure for reasons of clarity. (*D*) Close up view of the catalytic domain of VipD in ribbon diagram showing the surface clipped at the catalytic cleft. The surface is colored from white to green according to the Eisenberg hydrophobicity scale. (*E*) Superposition of the Rab5-GDP crystal structure [Protein Data Bank (PDB) ID code 1TU4] on the VipD:Rab5–GTP complex, illustrating the steric collision that prevents Rab-GDP from binding to VipD. The remainder of the VipD structure is omitted for clarity.

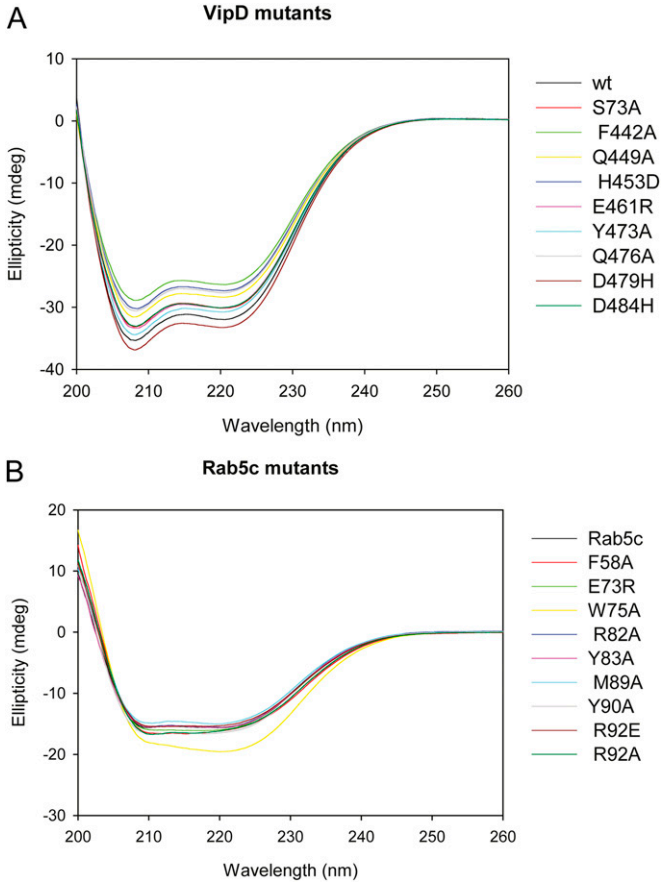

Fig. S2. Circular dichroism spectra of the the indicated wildtype and mutant proteins of (*A*) VipD and (*B*) Rab5c used in this study.

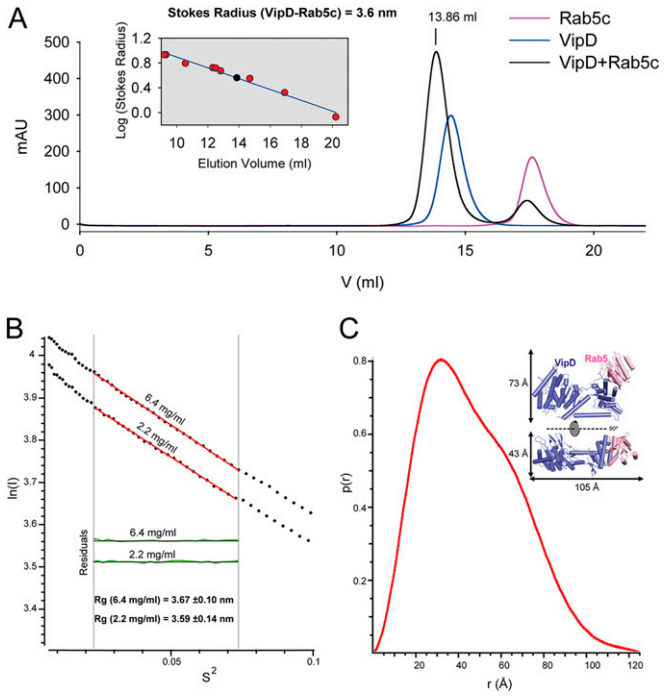

Fig. S3. Characterization of VipD–Rab5c complex in solution. (*A*) Analysis of the $VipD_{1–621}$–$Rab5c_{18–182}$ oligomeric state by gel filtration (Superdex 200 HR 10/30 column), leading to a Stokes radius estimation of ∼3.6 nm by comparison with the elution of model proteins (thyroglobulin, 8.5 nm; ferritin, 6.2 nm; γ-globulin, 5.3 nm; catalase, 5.2 nm; aldolase, 4.7 nm; BSA monomer, 3.5 nm; myoglobin, 2.1 nm; vitamin B12, 2.7 nm; *Inset*). Gel filtration of VipD (70 μM), Rab5c (140 μM), and VipD (70 μM) + Rab5c (140 μM). Note that the complex can be isolated using an excess of the Rab protein. (*B*) The guinier plot of the $VipD_{1–564}$–$Rab5c_{18–182}$ complex data at 2.2 and 6.4 mg/mL indicates a gyration radius of ∼3.6 nm. (*C*) This value is confirmed by the distance distribution function P(r), which suggests a bilobular structure with a radius of gyration of ∼36 Å and a maximum diameter of ∼120 Å fully compatible with the crystallographic structure of the VipD–Rab5c complex (*Inset*).

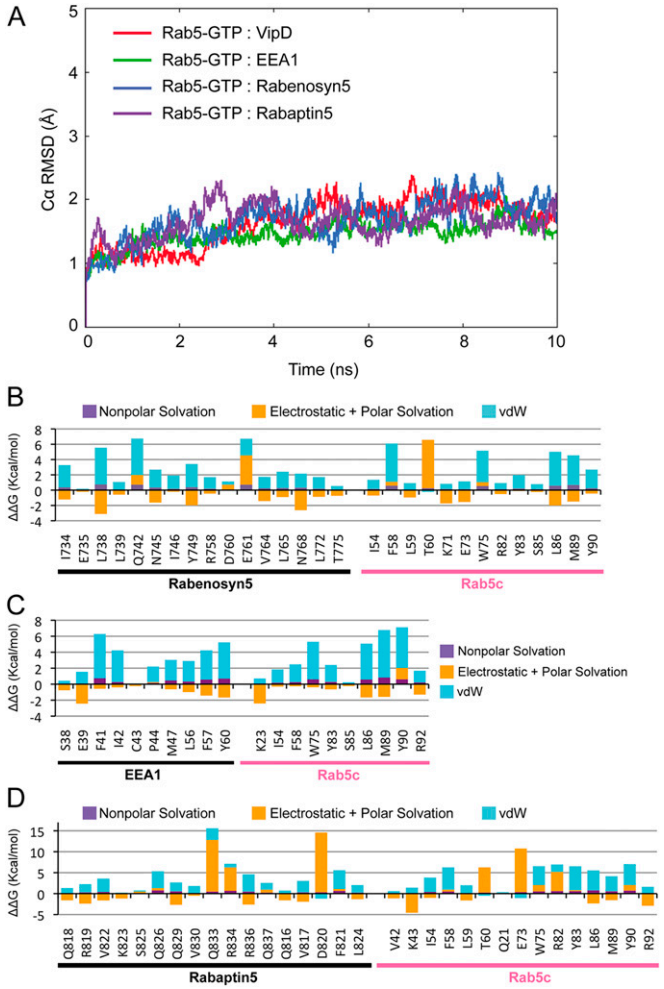

Fig. S4. (*A*) Plot of root mean square deviation (RMSD) relative to the coordinates of the initial (energy-minimized) structures during molecular dynamic simulations. (*B–D*) Per-residue contribution from van der Waals (vdW) energy (blue), nonpolar solvation energy (purple), and the sum of electrostatic and polar solvation energy (orange) calculated by computational alanine scanning for interfacial residues in the Rabenosyn5–Rab5c complex (*B*), EEA1–Rab5c complex (*C*), and Rabaptin5–Rab5c (*D*). Existing glycines and alanines are excluded in the calculation.

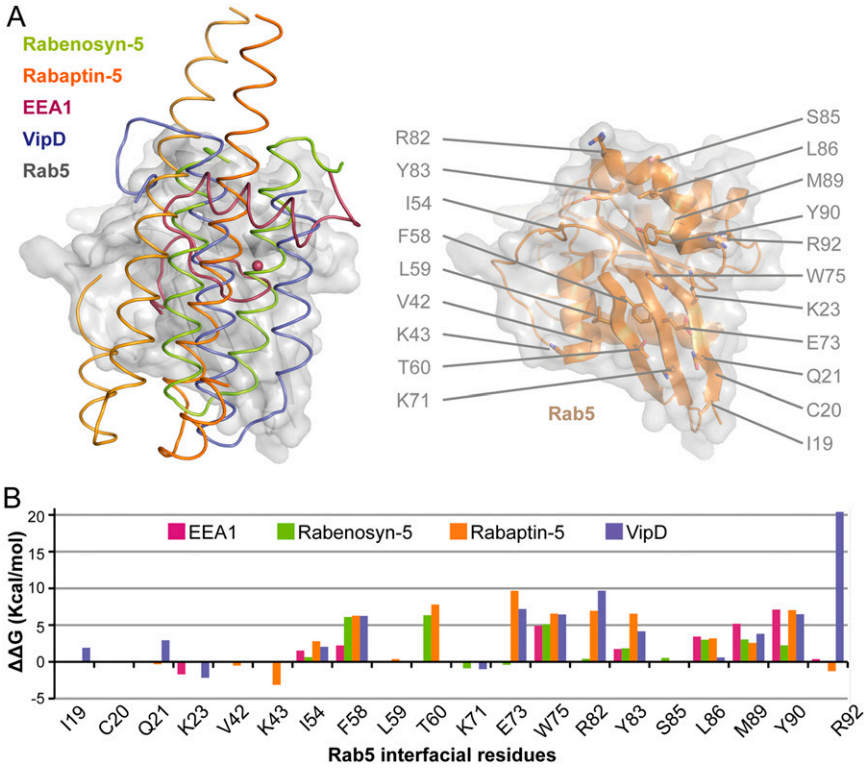

Fig. S5. (*A*) Superposition of effector binding epitopes in tube representation over Rab5c in transparent gray surface. EEA1 C2H2 Zinc Finger (PDB ID code 3MJH) in purple, Rabenosyn-5 (rebuilt from PDB ID code 1Z0J) in green, Rabaptin-5 (PDB ID code 1TU3) in orange, and VipD in slate. (*B*) Comparison of the ΔΔG values in the binding interface of Rab5c. Note that some residues at the preserved binding core show similar ΔΔG values, whereas other residues such as Arg92 constitute an effector-specific contact.

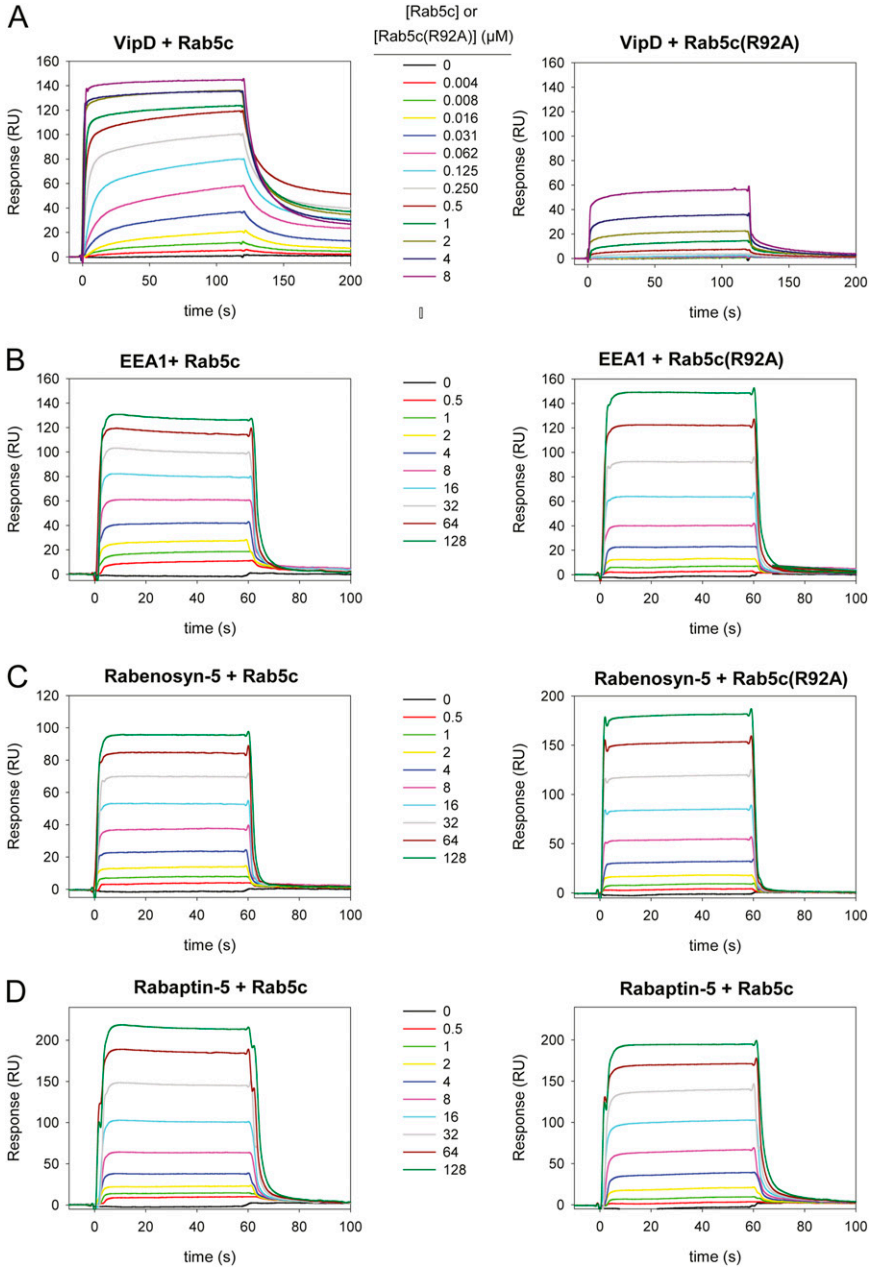

Fig. S6. Surface plasmon resonance (SPR) sensograms for binding of (*A*) VipD WT, (*B*) EEA1 C2H2 Zinc Finger [amino acids (aa) 36–91], (*C*) Rabenosyn-5 (aa 1–70), and (*D*) Rabaptin-5 (aa 739–862) to $Rab5c_{18–182}$(Q80L) (*Left*) or $Rab5c_{18–182}$(Q80L, R92A) (*Right*).

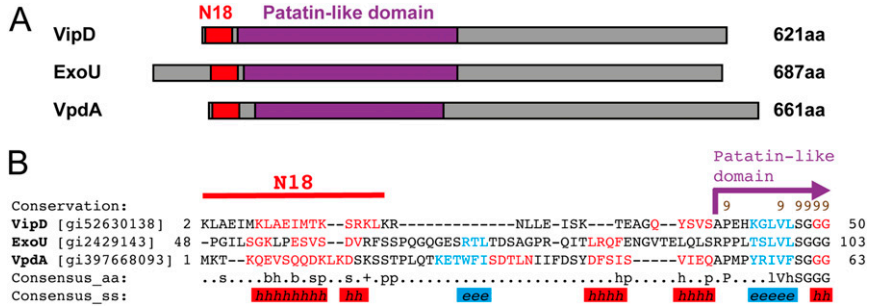

Fig. S7. The N-terminal tail of VipD shows structural similarity to equivalent regions in VpdA and ExoU. (*A*) Representative diagrams of VipD, VpdA, and ExoU highlighting the equivalent N-terminal tail. (*B*) PROMALS3D (PROfile Multiple Alignment with Predicted Local Structures and 3D Constraints) web server alignment (http://prodata.swmed.edu/promals3d/promals3d.php) of VipD, VpdA, and ExoU N-terminal regions.

Table S1. Plasmids used in this study

Plasmid	Properties	Reference
pGST-Parallel2-VipD(19-564)	Expression construct for N-terminal glutathione S-transferase (GST)-tagged *L. pneumophila* VipD domain covering residues 19–564 used for crystallization and PLA assays	This study
pGST-Parallel2-Rab5c$_{18–182}$ (Q80L)	Expression construct for N-terminal GST-tagged human Rab5c(Q80L) domain covering residues 18–182 used for crystallization, PLA assays and SPR assays	This study
pGST-Parallel2-VipD	Expression construct for N-terminal GST-tagged *L. pneumophila* VipD used for pull-down assays, PLA assays and SPR assays	This study
pGST-Parallel2-VipD(1-564)	Expression construct for N-terminal GST-tagged *L. pneumophila* VipD domain covering residues 1–564 used for PLA assays	This study
pGST-Parallel2-VipD(19-621)	Expression construct for N-terminal GST-tagged *L. pneumophila* VipD domain covering residues 19–621 used for PLA assays	This study
pGST-Parallel2-VipD(S73A)	Expression construct for N-terminal GST-tagged *L. pneumophila* VipD containing mutation S73A used for pull-down assays and PLA assays	This study
pGST-Parallel2-VipD(F442A)	Expression construct for N-terminal GST-tagged *L. pneumophila* VipD containing mutation F442A used for pull-down assays and PLA assays	This study
pGST-Parallel2-VipD(Q449A)	Expression construct for N-terminal GST-tagged *L. pneumophila* VipD containing mutation Q449A used for pull-down assays	This study
pGST-Parallel2-VipD(H453D)	Expression construct for N-terminal GST-tagged *L. pneumophila* VipD containing mutation H453D used for pull-down assays and PLA assays	This study
pGST-Parallel2-VipD(E461R)	Expression construct for N-terminal GST-tagged *L. pneumophila* VipD containing mutation E461R used for pull-down assays	This study
pGST-Parallel2-VipD(Y473A)	Expression construct for N-terminal GST-tagged *L. pneumophila* VipD containing mutation Y473A used for pull-down assays	This study
pGST-Parallel2-VipD(Q476A)	Expression construct for N-terminal GST-tagged *L. pneumophila* VipD containing mutation Q476A used for pull-down assays	This study
pGST-Parallel2-VipD(D479H)	Expression construct for N-terminal GST-tagged *L. pneumophila* VipD containing mutation D479H used for pull-down assays and PLA assays	This study
pGST-Parallel2-VipD(D484H)	Expression construct for N-terminal GST-tagged *L. pneumophila* VipD containing mutation D484H used for pull-down assays	This study
pGST-Parallel2-Rab5c$_{18–182}$	Expression construct for N-terminal GST-tagged human Rab5c(18-182) used for PLA assays	This study
pGST-Parallel2-Rab5c$_{18–182}$ (Q80L,F58A)	Expression construct for N-terminal GST-tagged human Rab5c(18-182) containing mutations Q80L and F58A used for pull-down assays and PLA assays	This study
pGST-Parallel2-Rab5c$_{18–182}$ (Q80L,E73R)	Expression construct for N-terminal GST-tagged human Rab5c(18-182) containing mutations Q80L and E73R used for pull-down assays	This study
pGST-Parallel2-Rab5c$_{18–182}$ (Q80L,W75A)	Expression construct for N-terminal GST-tagged human Rab5c(18-182) containing mutations Q80L and W75A used for pull-down assays	This study
pGST-Parallel2-Rab5c$_{18–182}$ (Q80L, R82A)	Expression construct for N-terminal GST-tagged human Rab5c(18-182) containing mutations Q80L and R82A used for pull-down assays	This study
pGST-Parallel2-Rab5c$_{18–182}$ (Q80L,Y83A)	Expression construct for N-terminal GST-tagged human Rab5c(18-182) containing mutations Q80L and Y83A used for pull-down assays	This study
pGST-Parallel2-Rab5c$_{18–182}$ (Q80L,M89A)	Expression construct for N-terminal GST-tagged human Rab5c(18-182) containing mutations Q80L and M89A used for pull-down assays	This study
pGST-Parallel2-Rab5c$_{18–182}$ (Q80L,Y90A)	Expression construct for N-terminal GST-tagged human Rab5c(18-182) containing mutations Q80L and Y90A used for pull-down assays	This study
pGST-Parallel2-Rab5c$_{18–182}$ (Q80L,R92E)	Expression construct for N-terminal GST-tagged human Rab5c(18-182) containing mutations Q80L and R92E used for pull-down assays	This study
pGST-Parallel2-Rab5c$_{18–182}$ (Q80L,R92A)	Expression construct for N-terminal GST-tagged human Rab5c(18-182) containing mutations Q80L and R92A used in SPR assays	This study

Table S1. Cont.

Plasmid	Properties	Reference
pGST-Parallel2-Rab22a$_{16–181}$ (Q64L)	Expression construct for N-terminal GST-tagged human Rab22a(16-181) containing mutation Q64L used in PLA and pull-down assays	This study
pGST-Parallel2-Rab7a(Q67L)	Expression construct for N-terminal GST-tagged human Rab7a containing mutation Q67L used in PLA assays	This study
pGST-Parallel2-EEA1$_{36–91}$	Expression construct for N-terminal GST-tagged human Rabenosyn5 domain covering residues 36–91 used in SPR assays	This study
pGST-Parallel2-Rabenosyn5$_{1–70}$	Expression construct for N-terminal GST-tagged human Rabenosyn5 domain covering residues 1–70 used in SPR assays	This study
pGST-Parallel2-Rabaptin5$_{739–862}$	Expression construct for N-terminal GST-tagged human Rabaptin5 domain covering residues 739–862 used in SPR assays	This study
pGST-Parallel2	Expression construct for GST used in SPR assays	(1)
pmCherry-C1	Mammalian expression vector generating an mCherry fusion to the N terminus of the protein of interest	Clontech (cat. 632524)
pmCherry-VipD	Expression construct generating an mCherry fusion to the N terminus of *L. pneumophila* full-length VipD	(2)
pmCherry-VipD(F442A)	pmCherry-VipD containing mutation F442A in the VipD-Rab5 interface	This study
pmCherry-VipD(H453D)	pmCherry-VipD containing mutation H453D in the VipD-Rab5 interface	This study
pmCherry-VipD(E461R)	pmCherry-VipD containing mutation E461R in the VipD-Rab5 interface	This study
pmCherry-VipD(Q476A)	pmCherry-VipD containing mutation Q476A in the VipD-Rab5 interface	This study
pEGFP-Rab5a(Q79L)	Expression construct generating a GFP fusion to the N terminus of human full-length Rab5a containing mutation Q79L generating constitutively active Rab5a	(3)

1. Sheffield P, Garrard S, Derewenda Z (1999) Overcoming expression and purification problems of RhoGDI using a family of "parallel" expression vectors. *Protein Expr Purif* 15(1):34–39.
2. Gaspar AH, Machner MP (2014) VipD is a Rab5-activated phospholipase A1 that protects Legionella pneumophila from endosomal fusion. *Proc Natl Acad Sci USA* 111(12):4560–4565.
3. Mattera R, Bonifacino JS (2008) Ubiquitin binding and conjugation regulate the recruitment of Rabex-5 to early endosomes. *EMBO J* 27(19):2484–2494.

Table S2. Oligonucleotides used in this study

Sequence	Plasmid	Cloning
TTTTTGGATCCGAAATATCAAAGACTGAGGCAGGACAATATTCTG	pGST-Parallel2-VipD(19-564)	BamHI/XhoI
TTTTTCTCGAGTCACGGTTCAGGTTGAACTTCAACTTTAAAGTCTTG		
TTTTTGGATCCAAGATCTGTCAATTTAAGCTGGTTCTGCTGGGGG	pGST-Parallel2-Rab5c$_{18–182}$(Q80L)	BamHI/XhoI
TTTTTCTCGAGTCAAAGCTTCTTAGCTATTGCCATGAAGATTTCGTTCACG		
TTTTTGGATCCATGAAACTTGCTGAAATTATGACAAAAAGCCGTAAATTAAAAAG	pGST-Parallel2-VipD	BamHI/XhoI
TTTTTCTCGAGTCAATGGCCGCCAAATGTGGTTGAAAGAC		
AATCTGACCCATGTTAGCGGAGCAGCAGCCGGAGCAATGACGGCGAGTAT	pGST-Parallel2-VipD(S73A)	SD
ATACTCGCCGTCATTGCTCCGGCTGCTGCTCCGCTAACATGGGTCAGATT		
GAGAAAGAGATTGCTGAGGCATCAGCGCATG	pGST-Parallel2-VipD(F442A)	SD
CATGCGCTGATGCCTCAGCAATCTCTTTCTC		
GAGATTTTTGAGGCATCAGCGCATGCAGCAGCTATTTTGCATCTTCAAGAACAAATCG	pGST-Parallel2-VipD(Q449A)	SD
CGATTTGTTCTTGAAGATGCAAAATAGCTGCTGCATGCGCTGATGCCTCAAAAATCTC		
GGCATCAGCGCATGCACAAGCTATTTTGGATCTTCAAGAACAAATCGTCAAAGAAATG	pGST-Parallel2-VipD(H453D)	SD
CATTTCTTTGACGATTTGTTCTTGAAGATCCAAAATAGCTTGTGCATGCGCTGATGCC		
GCTATTTTGCATCTTCAAGAACAAATCGTCAAACGAATGAATGATGGTGATTACAGTAG	pGST-Parallel2-VipD(E461R)	SD
GCTACTGTAATCACCATCATTCATTCGTTTGACGATTTGTTCTTGAAGATGCAAAATAGC		
GATGGTGATTACAGTAGCGTGCAAAATGCCTTAGATCAAATTGAAGACATTCTGACAG	pGST-Parallel2-VipD(Y473A)	SD
CTGTCAGAATGTCTTCAATTTGATCTAAGGCATTTTGCACGCTACTGTAATCACCATC		
GCGTGCAAAATTATTTAGATGCAATTGAAGACATTCTGAC	pGST-Parallel2-VipD(Q476A)	SD
GTCAGAATGTCTTCAATTGCATCTAAATAATTTTGCACGC		
CGTGCAAAATTATTTAGATCAAATTGAACACATTCTGACAGTCGATGCCAAAATGGATG	pGST-Parallel2-VipD(D479H)	SD
CATCCATTTTGGCATCGACTGTCAGAATGTGTTCAATTTGATCTAAATAATTTTGCACG		
AGATCAAATTGAAGACATTCTGACAGTCCATGCCAAAATGGATGACATCCAGAAAGAG	pGST-Parallel2-VipD(D484H)	SD
CTCTTTCTGGATGTCATCCATTTTGGCATGGACTGTCAGAATGTCTTCAATTTGATCT		
CAATTGGAGCGGCCGCACTCACACAGACTGTC	pGST-Parallel2-Rab5c$_{18–182}$(Q80L,F58A)	SD
GACAGTCTGTGTGAGTGCGGCCGCTCCAATTG		
CAACAGTCAAGTTTCGGATCTGGGACACAGC	pGST-Parallel2-Rab5c$_{18–182}$ (Q80L,E73R)	SD
GCTGTGTCCCAGATCCGAAACTTGACTGTTG		
CAAGTTTGAGATCGCGGACACAGCTGGACAG	pGST-Parallel2-Rab5c$_{18–182}$(Q80L,W75A)	SD
CTGTCCAGCTGTGTCCGCGATCTCAAACTTG		
GACACAGCTGGACTGGAGGCATATCACAGCCTGGC	pGST-Parallel2-Rab5c$_{18–182}$(Q80L, R82A)	SD
GCCAGGCTGTGATATGCCTCCAGTCCAGCTGTGTC		
GACACAGCTGGACTAGAGCGGGCTCACAGCCTGGCCCCCATG	pGST-Parallel2-Rab5c$_{18–182}$(Q80L,Y83A)	SD
CATGGGGGCCAGGCTGTGAGCCCGCTCTAGTCCAGCTGTGTC		
GAGCGGTATCACAGCCTGGCCCCCGCATACTATCGGGGGGCCCAGGC	pGST-Parallel2-Rab5c$_{18–182}$(Q80L,M89A)	SD
GCCTGGGCCCCCCGATAGTATGCGGGGGCCAGGCTGTGATACCGCTC		
GTATCACAGCCTGGCCCCCATGGCATATCGGGGGGCCCAGGCTGCC	pGST-Parallel2-Rab5c$_{18–182}$(Q80L,Y90A)	SD
GGCAGCCTGGGCCCCCCGATATGCCATGGGGGCCAGGCTGTGATAC		
TATCACAGCCTGGCCCCCATGTACTATGAAGGGGCCCAGGCTGCCATCGTGGTCTAT	pGST-Parallel2-Rab5c$_{18–182}$ (Q80L,R92E)	SD
ATAGACCACGATGGCAGCCTGGGCCCCTTCATAGTACATGGGGGCCAGGCTGTGATA		
TATCACAGCCTGGCCCCCATGTACTATGCGGGGGCCCAGGCTGCCATCGTGGTCTAT	pGST-Parallel2-Rab5c$_{18–182}$ (Q80L,R92A)	SD
ATAGACCACGATGGCAGCCTGGGCCCCCGCATAGTACATGGGGGCCAGGCTGTGATA		
TTTTTGGATCCGCGCTGAGGGAACTTAAAGTGTGCCTG	pGST-Parallel2-Rab22a$_{16–181}$ (Q64L)	BamHI/XhoI
TTTTTCTCGAGTCAGGATGGAATTCTTCGACTAATTTCTATAAAGAGTTC		
AAAAAACCATGGGAATGACCTCTAGGAAGAAAGTGTTGCTGAAGG	pGST-Parallel2-Rab7a(Q67L)	NcoI/XhoI
AAAAAACTCGAGTTAGCAACTGCAGCTTTCTGCCGAGGCC		
TTTTTGGATCCAGCTCTTCAGAGGGTTTCATATGTC	pGST-Parallel2-EEA1$_{36–91}$	BamHI/XhoI
TTTTTCTCGAGTTACTCTTGTCTGAGCAGTGTTACATC		
TTTTTGGATCCATGGCTTCTCTGGACGACCCAG	pGST-Parallel2-Rabenosyn5$_{1–70}$	BamHI/XhoI
TTTTTCTCGAGTTATGCTCGATCATCCCCTTCTCGT		
TTTTTCCATGGCTTCTATTTCTAGCCTAAAAGCTGAATTAG	pGST-Parallel2-Rabaptin5$_{739–862}$	NcoI/XhoI
TTTTTCTCGAGTCATGTCTCAGGAAGCTGGTTAATG		
AAAAGTCGACATGAAACTTGCTGAAATTATGACAAAAAGC	pmCherry-VipD	SalI/BamHI
AAGGATCCTTAATGGCCGCCAAATGTGGTTGAAAGAC		
GAAATCAGAGAAAGAGATTGCTGAGGCATCAGCGCATGCAC	pmCherry-VipD(F442A)	SD
GTGCATGCGCTGATGCCTCAGCAATCTCTTTCTCTGATTTC		
CATGCACAAGCTATTTTGGATCTTCAAGAACAAATCG	pmCherry-VipD(H453D)	SD
CGATTTGTTCTTGAAGATCCAAAATAGCTTGTGCATG		
CAAATCGTCAAAGAAATGAATCGTGGTGATTACAGTAGCGTG	pmCherry-VipD(E461R)	SD
CACGCTACTGTAATCACCACGATTCATTTCTTTGACGATTTG		
GTGCAAAATTATTTAGATGCAATTGAAGACATTCTGAC	pmCherry-VipD(Q476A)	SD
GTCAGAATGTCTTCAATTGCATCTAAATAATTTTGCAC		

SD, site-directed mutagenesis.